
Disentangled Planning and Control in Vision Based Robotics via Reward Machines

Alberto Camacho
Robotics at Google
albercm@google.com

Jacob Varley
Robotics at Google
jakevarley@google.com

Andy Zeng
Robotics at Google
andyzeng@google.com

Deepali Jain
Robotics at Google
jaindeepali@google.com

Atil Iscen
Robotics at Google
atil@google.com

Dmitry Kalashnikov
Robotics at Google
dkalashnikov@google.com

Abstract

In this work we augment a Deep Q-Learning agent with a Reward Machine (DQRM) to increase speed of learning vision-based policies for robot tasks, and overcome some of the limitations of DQN that prevent it from converging to good-quality policies. A reward machine (RM) is a finite state machine that decomposes a task into a discrete planning graph and equips the agent with a reward function to guide it toward task completion. The reward machine can be used for both reward shaping, and informing the policy what abstract state it is currently at. An abstract state is a high level simplification of the current state, defined in terms of task relevant features. These two supervisory signals of reward shaping and knowledge of current abstract state coming from the reward machine complement each other and can both be used to improve policy performance as demonstrated on several vision based robotic pick and place tasks. Particularly for vision based robotics applications, it is often easier to build a reward machine than to try and get a policy to learn the task without this structure.

1 Introduction

Deep reinforcement learning (RL), and in particular DQN, has proven success across different domains (e.g. playing Atari games from pixels [23], playing board games [28], and doing control from raw pixel observations in robotics applications [17]). The main practical advantage of DQN over tabular methods resides in the capability of neural networks to generalize during inference. Despite apparent success, it has been widely recognized that deep RL methods are sample inefficient, and they often require heavy training to reach an acceptable quality. To mitigate for this, it is common in robotics to provide the RL agent with a set of *demonstrations* (that can be used for doing imitation learning and bootstrapping DQN), heuristics, and additional rewards to further guide exploration.

We evidence an important limitation of standard DQN, caused by having to solve two related subproblems: 1) learning latent state features, and 2) learning a policy that is conditioned on such features. DQN solves the two subproblems at once, while we show value in decoupling them. Intuitively, some of these features describe state properties at an abstract level and may be indicative of the current stage of a task. This collection of features defines an abstract state, a notion that can be exploited to decompose long-horizon tasks into simpler subtasks. Not surprisingly, abstract states are an additional supervision signal that complement rewards in RL. Our main insight is in revealing how crucial an explicit notion of abstract states can really be. Even in very simple tasks, DQN failed to learn good-quality policies unless abstract states were provided. This phenomenon occurs even when the information encoded in abstract states was already contained within state observations.

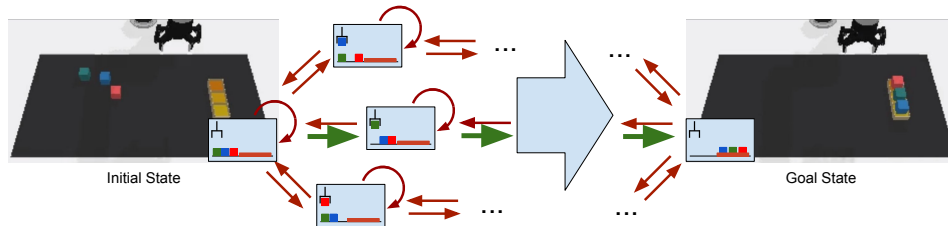


Figure 1: System Overview. Initial and goal states show the starting scene configuration and desired goal configuration. These map to abstract states within the reward machine (light blue boxes). In this example, abstract states are determined by the value of 15 boolean features representing whether or not various blocks are on the table, in different parts of the container, or in the gripper. In our work, the agent is provided a one-hot encoding of the current abstract state (not with the boolean features). Green arrows show the shortest path through the reward machine to reach the goal state. Red arrows illustrate a sample of the many transitions between abstract states within the reward machine.

We address the two subproblems mentioned above by taking a hybrid approach to reinforcement learning, where the agent has access to a set of *feature detectors*. State features enable the agent to keep track of which abstract state is at. This way, policies need be conditioned on fewer latent features and are easier to learn. Then, we construct dense reward functions that facilitate learning sub-policies conditioned on abstract states. Our approach makes use of *reward machines*, a mathematical structure that provides a principled mechanism to drive the agent along different abstract states, and equips them with a dense reward structure that guides exploration toward task completion [30]. We show how to construct a reward machine from demonstrations, in a way that it centers Q values around zero—which is beneficial to deep learning methods.

Our experiments evidence the limits of standard DQN, which was unable to learn good-quality policies even in very simple vision-based robotics tasks. We also showcase how reward machines help overcome such limitations. Reward machines provide supervision signals coming from abstract states and reward shaping. Abstract states (resp., rewards) alone can be effectively exploited by DQN to improve on sample efficiency and policy quality, but it is in the combination of using abstract states and rewards together that DQN manifests a substantially improved performance.

This work concludes that, in certain applications, augmenting the agent with meaningful abstract state features can drastically improve policy learning. Conversely, failing to provide the agent with this additional structure may prevent DQN from learning good policies *even in very simple tasks*. Abstract state representations can be learned [21], but doing so may not even be needed in practice. In a number of robotic applications it is easy to obtain abstract state representations by hand—e.g., by extracting features from a depth camera, or the pose of the end effector. Our work evidences the practicality of reward machines in vision-based manipulation tasks, and opens the door to future research directions to better design and exploit reward machines.

Running example (kitting task). Consider a pick & place kitting task, in which a robotic arm has to place three blocks of different colors in their designated plate inside of a container (Figure 1). Given a robot with depth cameras, it is feasible to engineer feature detectors that detect whether the end effector is holding a block, the color of such block, and whether a block of certain color is on the table (resp., on their designated plate). The value of state features can be used to solve this task at an abstract level—e.g., if one block is not on their designated plate, then *pick up* such block; if the end effector is holding a block, then *place* it on their designated plate. However, state features alone are not sufficient to solve the task, because block locations are relevant to determine (low-level) actions. Despite the features alone are not sufficient, their truth values are indicative of task progression.

2 Related Work

Task Decomposition in RL reduces complex tasks into simpler subtasks that an agent can learn independently and in parallel—which results in more efficient learning [18]. Hierarchical RL (HRL) is one such framework that decomposes planning and control into two alternating levels: 1) a high-level policy that transforms observations into temporally extended actions, and 2) low-level policies (conditioned on high-level actions) that execute for a specified amount of time before control returns

to the high level. Recent options-based methods [29] learn options from reference data [22, 25] through interactions with the environment [9, 8]. Designing good options still requires substantial manual engineering and hand tuning, and is difficult to scale as the complexity of the task increases.

State Abstractions are used to reduce the search space in MDPs, by aggregating states that share certain properties in common. A number of techniques have been studied to compute and learn MDP abstractions [21, 2]—e.g., bi-simulations [12]—, with trade-offs between state compression and RL performance [1]. In this work, we are not concerned with planning in the abstract state. Rather, we augment state observations with abstract states, and examine to which extent they are a useful (and sometimes, crucial) extra supervision signal for deep RL.

Reward Machine (RM) is a framework that decomposes complex tasks into finite-state machines that encode reward functions for MDPs [30]. An RM is characterized by a set of internal abstract states that form a graph, in which the agent navigates through different modes of operation. Transitions between abstract states indicate different sub-policies, each associated with an individual reward function. The graph structure of RMs can be exploited toward more sample-efficient RL [30, 7, 31]. The abstract states of an RM do not necessarily need to be directly correlated with the progression of any one specific task. This property makes them practical to use for real robot systems, with which various simple hardware signals can be used as features—e.g., end effector states, gripper opening, suction flow sensor readings, proximity sensor readings, joint encoders, etc.

RL for Vision-Based Manipulation policies that map pixels to actions have shown promise for of tasks including grasping [17, 32, 20, 19, 33], stacking [36], pushing [26], tossing [35], and even a Rubik’s cube [3]. Many of these vision-based RL systems leverage handcrafted features beyond pure rgb observations. For example, the gripper height and status [17], a hash of the current state [10], and a CNN prediction of the current pose and state of the cube [3]. Beyond just incorporating additional features into the observation, we demonstrate RMs as a principled and effective means to integrate additional state features to improve the learning efficiency of RL for manipulation tasks.

3 Background

A *Markov Decision Process* (MDP) is a tuple $\langle S, s_0, T, A, r, \gamma \rangle$, where S is a set of states, and $s_0 \in S$ is the initial state. RL agents interact with an MDP by performing *actions*, from the set A . As a result of performing action $a \in A$ in state s , the state is updated to some $s' \in S$ according to the probability distribution $T \sim T(s, a)$. Upon transitioning to s' , the agent receives a reward signal $r(s, a, s') \in \mathbb{R}$. RL agents do not know the model, but can *sense* the state to obtain an observation $obs(s)$ that may or may not fully describe s , and that may or may not be noisy. The objective of the agent is to learn a policy π , or a mapping from state observations into action distributions, that maximizes the expected cumulative discount value $V_\pi(s_0) = \mathbb{E}_\pi \sum \gamma^t r(s_t, a_t, s_{t+1})$ s.t. $a_t \sim \pi(obs(s_t))$. The discount factor $0 < \gamma \leq 1$ incentivizes the agent to accrue reward early on. For simplicity, in the sequel we consider fully observable MDPs where $obs(s) = s$. In this paper we address **behavioral MDPs** in which the objective is to complete a task, and policy execution terminates upon task completion. Those states for which the task is completed are denoted as *goal* states. Rewards in behavioral MDPs are designed so that optimizing $V_\pi(s_0)$ is correlated with optimizing for task completion—e.g., rewards can be 1 in transitions to goal states, and zero otherwise. We presume that the environment is reset after the task is completed, or after the number of steps in the current episode surpasses a fixed threshold.

Deep Q learning for MDPs (DQN). Q learning is a model-free RL method that computes a policy π by learning a Q function q_π over state-action pairs (s, a) that estimates the expected cumulative reward of performing a in s , and acting according to π thereafter. Policy $\pi(s)$ follows a probability distribution over actions induced by $q_\pi(s, \cdot)$ —e.g., a *greedy* policy $\pi_{greedy}(s) = \arg \max_a q(s, a)$. Q learning interleaves exploration with training. Usually, exploration is performed with an epsilon-greedy policy, and experience tuples (s, a, r, s') are stored in an *experience replay* buffer. Training steps update the incumbent Q function q by sampling batches of experience, and performing the updates $q(s, a) \leftarrow \alpha(r(s, a, s') + \max_{a'} \gamma q(s', a')) + (1 - \alpha)q(s, a)$ for some learning rate α . In behavioral MDPs, we define $q(s, \cdot) := 0$ in goal states. The greedy policy π_{greedy} is guaranteed to converge to optimal, provided that all state-action pairs are visited infinitely often, and Q values are updated infinitely often. *Deep Q learning* (DQN) extends Q learning with a neural network that acts as Q function approximator [23]. DQN does not have optimality guarantees, but in practice it can scale to larger problems than Q learning thanks to the the inference capabilities of neural networks.

Reward machines. Formally, a RM is a tuple $\langle U, u_0, \Sigma, \delta, \rho \rangle$, where U is a set of RM states, and u_0 is the initial state. A RM operates in an MDP $\langle S, s_0, T, A, r, \gamma \rangle$. In this paper, $\Sigma = S$ is the set of state observations in the MDP. The RM issues reward signal in response to MDP transitions (s, a, s') , that depends on their current internal state u . More precisely, such reward is $\rho_u(s, a, s') \in \mathbb{R}$. Upon observing a symbol $s' \in \Sigma$, the RM transitions to a new state $u' = \delta(u, s')$. The mechanics of a RM together with the MDP are equivalent to the mechanics of a *cross-product* MDP $M' = \langle S', s'_0, T', A, r', \gamma \rangle$, defined in the natural way. The set of states is $S' = S \times U$, and $s'_0 = (s_0, u_0)$. The transition of state $((s, u), a)$ by action a is a state (s', u') , where $s' \sim T(s, a)$ follows the distribution in the original MDP and $u' = \delta(u, s')$ is a transition in the RM. Finally, the reward function adds up the rewards coming from the original MDP and the RM. More precisely, $r'((s, u), a, (s', u')) = r(s, a, s') + \rho_u(s, a, s')$. For more detailed information, we refer to [30].

Q learning for RMs (QRM). Whereas the cross-product of an MDP with a RM is a standard MDP that can be handled by standard methods, the graph structure of RMs can be exploited with dedicated algorithms. In particular, *Q learning with RMs* (QRM) and *Deep QRM* (DQRM) showed an improved sample efficiency over Q learning [30]. The benefits of QRM and DQRM were shown, mostly, in MDPs with non-Markovian rewards, discrete state features, and discrete actions. Their major trick is that they *broadcast* experience to all RM states. More precisely, experience is obtained by interacting with the original MDP, and each individual experience (s, a, s') is used to generate *multiple* experience tuples in the cross-product MDP: $((s, u), a, (s', u'))$ for each RM state u and RM transition to u' . It is worth noting that broadcasting experience pays off in RMs where the agent may visit the same state s in different RM states. This is likely to occur in RMs that encode *non-Markovian rewards*, but it is less apparent in MDPs for Markovian tasks. In this work, we show that RMs can be also used for task decomposition in Markovian tasks, and they have extra benefits beyond broadcasting experience. Furthermore, we show that RMs can be also effective in vision-based tasks with large action spaces, which were not evaluated in previous related work.

4 Deep Q-Learning with Reward Machines (DQRMs) from Demonstrations

In this and the following sections we address the problem of designing a reward function for behavioral MDPs. The problem can be recast as designing a RM that operates in conjunction with an MDP that has zero constant rewards. Constructing RMs requires a thought process to ensure that the graph structure captures task progression, and the reward function provides guidance and induces the desired behavior—similar to the process of designing reward functions, actions, and state spaces for standard MDPs. In order to facilitate such endeavor, recent work introduced principled methods to construct RMs from a high-level logical specification of the intended behavior of the agent [7].

In this section we present a method to construct RMs from demonstrations. Demonstrations are sequences of states s_0, s_1, \dots, s_n that show how a certain task—e.g., stacking a tower of blocks—can be completed, ending in one of the *goal* states. Demonstrations can be often acquired with a minimal technical knowledge, compared to constructing RMs by hand or designing logical specifications.

4.1 Constructing RMs from Demonstration

RMs can be constructed from a set of demonstrations in two stages. First, we construct an *abstract planning graph*. In a second stage, we equip such graph with a reward function to obtain a RM. We introduce the necessary concepts below. In the following, we presume that the agent has access to a set of *feature* detectors. Features are associated with properties that can hold in state observations. Formally, features are boolean propositions, and we denote the set of features with AP—which stands for *atomic propositions*. Let $F : S \rightarrow 2^{AP}$ be the function that maps state observations s into the subset $\sigma \subseteq AP$ of features that hold true in s . We say that $\sigma = F(s)$ is the *abstraction* of state s in AP by F . We further presume that the set of features are rich enough to discriminate between goal and non-goal states—i.e., goal and non-goal states must be mapped into different abstract states. For convenience, we say that an abstract state is a goal if it is the abstraction of some goal state.

Stage 1: Constructing an abstract planning graph. The *abstract demonstration* associated to a demonstration s_0, s_1, \dots, s_n is a sequence $\sigma_0, \sigma_1, \dots, \sigma_n$, where σ_i is the abstraction of s_i into AP by F , for each $i \in \{1, \dots, n\}$. A set of demonstrations defines the *abstract planning graph* (V, E) as follows. The set of nodes, V , is the set of abstract states σ that appear in the abstract demonstrations. The set of directed edges, E , connect σ with σ' if, and only if, σ and σ' are two consecutive abstract

states in some abstract demonstration. It is worth noting that our construction presumes that the task is Markovian, and goal states do not depend on the past history. In the general case, our methods could be used in conjunction with existing methods that construct graph-like structures (such finite-word automata and Moore machines) that capture non-Markovian behavior (e.g., [11, 6]).

Stage 2: Constructing a RM. The planning graph gives us almost all the ingredients to construct a RM $\langle U, u_0, \Sigma, \delta, \rho \rangle$. The set of RM states, U , is the set of abstract states 2^{AP} ; the initial state of the RM is the abstraction of the initial state s_0 of the MDP, i.e., $u_0 = F(s_0)$; the input alphabet, Σ , is the set of states S ; the transition function simply maps observations into abstract states, i.e., $\delta(u, s) = F(s)$; finally, the reward function $\rho_u(s, a, s') = \mathbb{1}_{goal}(s')$ is the *indicator* function that evaluates to 1 if s' is a goal, and zero otherwise. We have the following property:

Property 1 *The RM constructed with the method described above assigns reward 1 to MDP executions that achieve the goal, and zero otherwise.*

Running example (cont.) In the kitting task utilized in this work, RM states are abstractions that indicate whether or not the gripper is holding a block of certain color, and whether or not such blocks are placed on their designated plate (resp., on the table). Features can be obtained by handcrafting heuristics, or training CNN’s to detect either the presence or pose of objects specific to a task. Figure 1 shows a planning graph for this task. RM states correspond to the nodes of such graph, depicted with sketches of the features. In our task, all goal states abstract to the same RM state. The reward function $\rho_u(s, a, s') = \mathbb{1}_{goal}(s')$ evaluates to 1 when the observation s' abstracts to a goal state.

5 Inducing Zero-Valued Optimal Q Values With Dense Rewards

The behavioral MDP constructed with the RM in Section 4 has very sparse rewards. In this section we construct RMs with denser rewards that can provide better guidance, via *reward shaping*. Reward shaping is a technique that transforms the reward function r in MDPs, with the purpose of obtaining a new MDP that can be better handled by RL and planning methods [24]. The new MDP looks the same as the original, except for their reward function r' . Reward shaping in infinite-horizon discounted MDPs preserves optimal solutions when reward transformations are a difference of *potentials*—i.e., $r'(s, a, s') = r(s, a, s) + \gamma Pot(s') - Pot(s)$ for some bounded *potential* function $Pot : S \rightarrow \mathbb{R}$. We use the reward transformation presented in [5, 7], which simply involves modifying the reward function of the RM, ρ , with an auxiliary function $Pot : U \rightarrow \mathbb{R}$, that assigns potentials to RM states.

$$\rho'_u(s, a, s') = \rho_u(s, a, s') + \gamma Pot(u') - Pot(u), \text{ where } u' = \delta(u, s')$$

In addition, we require $Pot(u) = c$ be constant in goal states. When we apply such reward shaping to the behavioral MDP M constructed in Section 4, we obtain a new behavioral MDP M' with a denser reward function r' that preserves optimal and sub-optimal solutions (Theorem 1). This property follows by analyzing the telescopic sum of rewards of policy executions in M' —which have finite or infinite length depending on whether the goal is achieved or not, respectively. The former case simplifies to $\sum_0^{n-1} \gamma^k r'(s_k, a_k, s'_{k+1}) = -Pot(u_0) + \gamma^n c + \gamma^{n-1}$, and the latter simplifies to $\sum_0^\infty \gamma^k r'(s_k, a_k, s'_{k+1}) = -Pot(u_0)$. Compared to the rewards if executions M : (i) rewards to executions that achieve the goal are rescaled from 1 to $c + 1/\gamma$; and (ii) execution rewards are uniformly affected by a constant offset, $-Pot(u_0)$. Either transformation preserves optimal solutions.

Theorem 1 *Potential-based reward shaping in discounted behavioral MDPs preserves optimal and near-optimal solutions, provided that the potentials in RM goal states are constant.*

Optimal Reward Shaping We now show how to choose a suitable potential function, $Pot^*(u)$, when the two properties stated in Theorem 2 (they hold in our running example). We do it in a way that, by construction, the optimal Q values in M' evaluate to zero in all states—i.e., $\max_a q^*(s, a) = 0$ in all s . In non-goal states, we set $Pot^*(u) = \gamma^{dist(u)}$, where $dist(u)$ is the minimal distance from u to a goal state in the abstract planning graph, and γ is the MDP discount factor. In goal states, we set $Pot^*(u) = c$ with c so that $1 + \gamma c = \gamma$. In practical terms we are forcing that the combination of the rewards coming from ρ and ρ' behaves as if the MDP M' had rewards coming from only a single RM with potentials $Pot^*(u) = \gamma^{dist(u)}$, also in goal states—i.e., $\gamma Pot^*(u) = 1$ in goal states.

The MDP M' with potential function $Pot^*(u) = \gamma^{dist(u)}$ has, by construction, an optimal value function $V^*(s) := \max_a q^*(s, a) = 0$ (Theorem 2). This is because the immediate rewards for

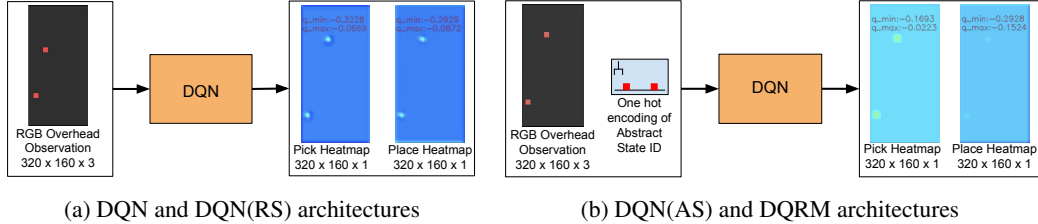


Figure 2: Overview of different architectures. Figure 2a shows a vanilla DQN architecture, used by DQN and DQN(RS), which takes RGB top down images as observations. In DQN and DQN(RS), the RM is used to compute the rewards received by the agent. Figure 2b shows the architecture used by DQN(AS) and DQRM, which take observations augmented with the current RM state.

optimal actions in M' are zero ($\gamma Pot^*(u') - Pot^*(u) = 0$). The same potential function Pot^* had been used in [7], but the their properties on translating optimal Q values to zero were not identified.

Theorem 2 *Potential-based reward shaping in the MDP M with $Pot(u) = \gamma^{dist(u)}$ as described above results in an MDP M' with zero-valued optimal Q values, provided that: (i) all feasible RM transitions can be realized with a single action of the MDP; and (ii) all feasible RM transitions can be realized deterministically, by choosing the right action.*

We observe that doing RL in an MDP whose optimal Q values are zero can be advantageous, especially to *deep* RL approaches. Bringing target Q values within a range around 0 benefits training very large DQNs, as it reduces the Internal Covariate Shift from gradient descent optimization [16, 4]. This leads to more stable training since smooth L1 loss gradients are thereby less likely to excessively perturb convolutional network weights [27].

Running example (cont.) In the kitting task, with planning graph illustrated in Figure 1, we can assign potentials to RM states according to their distance to a goal state. For example, a state s that has two blocks placed in their designated plate (and the third block is on the table) is two steps away from the goal, and has potential $Pot^*(F(s)) = \gamma^2$. Moving optimally from this state (i.e., picking up the remaining block) results in a reward 0. Sub-optimal moves incur in a negative reward.

6 Experimental Results

We evaluated the benefits of our methods for task decomposition in two *pick & place* tasks. The first task consists on stacking a tower of two red blocks. The second task is the kitting task, with three blocks of different colors, discussed in our running example. Blocks are initially placed in random locations. Our environment is simulated in PyBullet, and consists of a *Universal Robot 5* (UR5) grasping arm, a plane, and several blocks of different colors that vary with the task. The robot is equipped with RGB and depth cameras with top-down views of the working area. Observations are RGB images with 320x160 pixels per channel. The robot can perform *pick* and *place* actions, parameterized with the pixel coordinates (x, y) of the target location of the end effector. The depth camera senses the depth of the objects in the scene, and is used to compute the height z of the target location. In all our tasks, we constructed reward machines from demonstrations, as explained in previous sections, and with the help of feature detectors that were hardcoded.

We implemented different versions of DQN in TF-agents [13], that we detail below and illustrate in Figure 2. In all cases, the DQN consists of two independent feed-forward 43-layer residual networks (ResNets) [14]. This architecture has previously been shown to improve learning efficiency for vision-based DQNs [36, 15, 34]. Q predictions are optimized towards target Q values with Huber loss. Batch training was performed by sampling evenly from an experience replay buffer of size 1000, and a buffer of size 1000 fulfilled with demonstrations. Additional details in the Appendix.

- DQN: The standard version of DQN, with rewards 1 in transitions to goal states.
- DQN(RS): DQN with the dense reward shaping provided by the RM.
- DQN(AS): DQN with observations augmented with the RM state (abstract state).
- DQRM: The combination of DQN(AS) and DQN(RS).

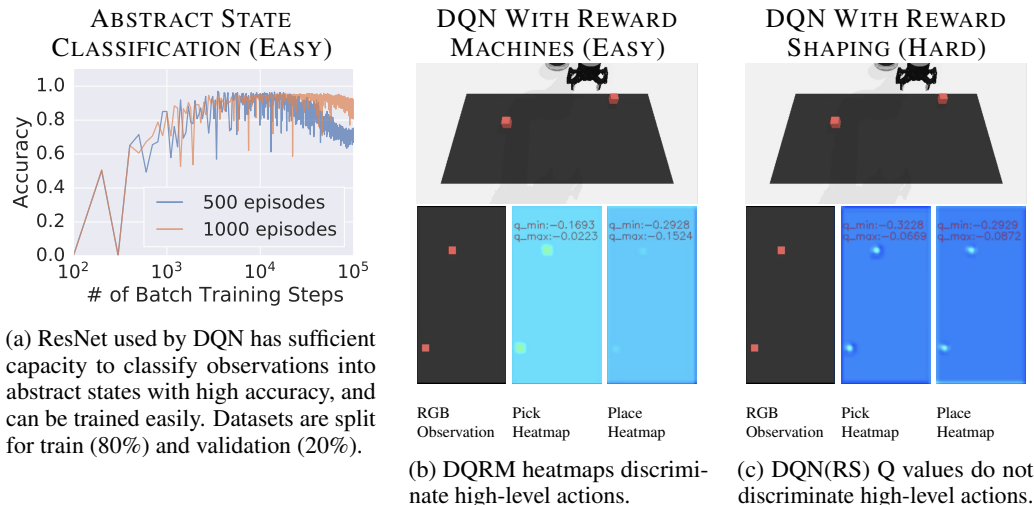


Figure 3: Abstract states are useful state features that help DQN disentangling planning and control. DQN can find it challenging to learn a policy that conditions actions on abstract state features, even when learning those features is an easy classification task (Figure 3a). DQRN takes abstract states as part of the input, and is able to make a clear distinction on the right high-level action *pick* (planning) and their low-level parameters (control). DQN(RS) does not take abstract states as part of the input, and cannot discriminate between high-level actions (Figure 3c). The low performance in DQN(RS) is not due to the lack of capacity of the neural network, nor to the difficulty of the classification task.

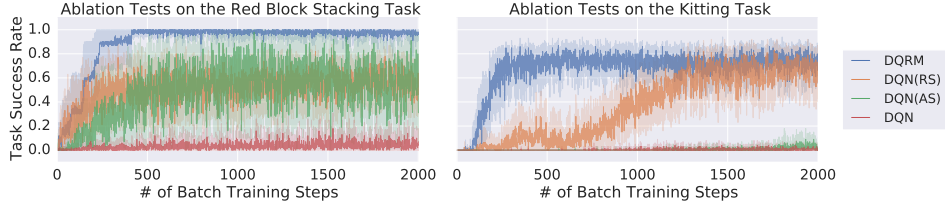
6.1 Disentangled Planning and Control

We evidenced some of the limitations of DQN. When actions are highly conditioned on high-level state features, DQN may not be successful at disambiguating between states that differ at an abstract level. Our tests consist of a very simple stacking blocks task: when there are two blocks on the table, the agent should pick up one block; when there is one block on the table, the agent should place the block it’s currently holding on top of the other block. The problem is that when training DQN, the ResNet network cannot distinguish between observations in which there is only one block on the table (the optimal action is *place*) from observations in which there are two blocks on the table (the optimal action is *pick*). The agent perceives that *sometimes* the good action is *pick*, and *sometimes* is *place*, and that in all cases the target location of the gripper is a red block. In Figure 3c we see this phenomenon: the Q value heatmaps for the pick and place actions look very similar. As a sanity check, we assessed that the low performance of DQN was not due to a limited capacity of the ResNet network. Figure 3a evidences that that this is not the case, and the ResNet can be trained to classify observations into abstract states. Moreover, it appears that the classification task is easy.

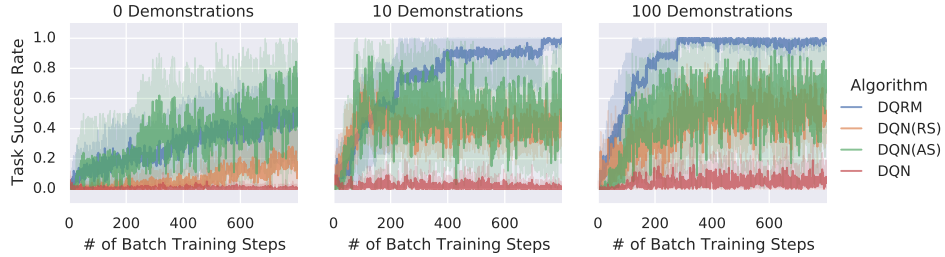
Figure 3b shows that DQRN can successfully disambiguate between abstract states, and output optimal actions. This is because good-quality policies need be conditioned in fewer latent features, given the current abstract state. It appears that classifying observations into abstract states is easy, and RL given abstract states is also easy, but the combined task of learning policies without abstract states is significantly more difficult. RMs and DQRN make the combined task easy.

6.2 Evaluating the Benefits of RMs for Task Guidance

RMs provide the agent with two sources of guidance (abstract states and reward shaping) that complement each other. Reward shaping induces a denser reward structure that can improve guidance. In our experiments (see Figure 4a), DQN(RS) greatly outperformed standard DQN. Abstract states help correlate optimal actions with observations, In the red block stacking task, DQN(AS) was successful in doing so thanks to the short makespan of the task (two steps). However, abstract states alone were not beneficial to DQN(AS) in the kitting task (which has a longer makespan of six steps). A great result in our experiments is that the two sources of guidance mentioned above complemented each other. We see this in DQRN, whose performance greatly outperforms the performance of all other configurations. While DQN(RS) needed 1,500 batch training steps



(a) Ablation tests of different versions of DQN on two pick & place tasks. The abstract state variables and reward shaping of our DQRM approach provide guidance and greatly improve the performance of DQN.



(b) Impact of the number of demonstrations (0, 10, and 100) in the performance, evaluated on the block stacking task. DQRM is the configuration that best exploits the guidance in demonstrations.

Figure 4: Success rate vs. number of episodes for different versions of DQN, trained in batches of size 64 at the end of each episode. Results are averaged over 10 experiments, and 10 evaluation runs per datapoint. Abstract states, reward shaping, and demonstrations provide useful supervision.

to achieve an acceptable success rate, DQRM needed only 200 batch training steps. Furthermore, DQRM could learn better-quality policies with fewer batch training steps, and their success rate is more stable.

6.3 Exploiting RMs and Demonstrations

In robotics applications it is common to use a set of expert demonstrations, in conjunction with exploratory data, to help training DQN. DQRM can also benefit from demonstrations (see Figure 4b). In our tests on the stacking blocks task, we only needed to provide DQRM with a handful of them (10) to see a significant performance increase. Batch training samples evenly from the demonstration and exploration buffers, and good-quality demonstrations successfully bias learning. We only needed about 100 demonstrations to reach a peak of performance in DQRM, comparable to training with 500 demonstrations (see Figure 4a left). Without demonstrations, the configuration that performed best is DQN(AS), with high variance compared to DQRM. However, once some demonstrations are provided to the agent, the performance DQRM greatly outperformed others.

7 Conclusion

This work illustrates the benefits of using reward machines in vision based robotic manipulation tasks with large action spaces, and how they help overcome the limitations of DQN. We analyze two related subproblems that make training DQN policies difficult: learning meaningful latent state features, and learning a policy that is conditioned on such features. Providing the agent with the abstract state helps disentangle planning and control, and the resulting policies are easier to train. Reward machines provide the mathematical structure to manage abstract states in a principled manner, while also providing a dense reward function to give guidance toward task completion. Whereas constructing reward machines by hand can be impractical, we show how to construct them from a set of demonstrations that can also be leveraged to bootstrap DQRM. Either abstract states or dense reward shaping alone can be exploited to improve on sample efficiency and policy quality. Notably, DQRM manifests a substantially improved performance with the combination of using both abstract states and rewards together. In some cases, DQRM learns good-quality policies with less than 2000 batch training steps, while the sole use of either abstract states or dense reward shaping alone requires 1,500 batch training steps to asymptotically converge to policies that have worse quality.

References

- [1] David Abel, Dilip Arumugam, Kavosh Asadi, Yuu Jinnai, Michael L. Littman, and Lawson L. S. Wong. State abstraction as compression in apprenticeship learning. In *Proceedings of the 33rd AAAI Conference on Artificial Intelligence (AAAI)*, pages 3134–3142, 2019.
- [2] David Abel, D. Ellis Hershkowitz, and Michael L. Littman. Near optimal behavior via approximate state abstraction. In *Proc. 33rd Intl. Conf. on Machine Learning (ICML)*, pages 2915–2923, 2016.
- [3] Ilge Akkaya, Marcin Andrychowicz, Maciek Chociej, Mateusz Litwin, Bob McGrew, Arthur Petron, Alex Paino, Matthias Plappert, Glenn Powell, Raphael Ribas, et al. Solving rubik’s cube with a robot hand. *arXiv preprint arXiv:1910.07113*, 2019.
- [4] Jimmy Lei Ba, Jamie Ryan Kiros, and Geoffrey E Hinton. Layer normalization. *arXiv preprint arXiv:1607.06450*, 2016.
- [5] Alberto Camacho, Oscar Chen, Scott Sanner, and Sheila A. McIlraith. Non-markovian rewards expressed in LTL: guiding search via reward shaping. In *Proceedings of the 10th International Symposium on Combinatorial Search (SoCS)*, pages 159–160, 2017.
- [6] Alberto Camacho and Sheila A. McIlraith. Learning interpretable models in linear temporal logic. In *Proceedings of the 29th International Conference on Automated Planning and Scheduling (ICAPS)*, pages 621–630, 2019.
- [7] Alberto Camacho, Rodrigo Toro-Icarte, Torny Q. Klassen, Richard Valenzano, and Sheila A. McIlraith. LTL and beyond: Formal languages for reward function specification in reinforcement learning. In *Proc. of the 28th Intl. Joint Conf. on Artificial Intelligence (IJCAI)*, pages 6065–6073, 2019.
- [8] John D. Co-Reyes, Yuxuan Liu, Abhishek Gupta, Benjamin Eysenbach, Pieter Abbeel, and Sergey Levine. Self-consistent trajectory autoencoder: Hierarchical reinforcement learning with trajectory embeddings. In *Proc. of the 35th Intl. Conference on Machine Learning, (ICML)*, pages 1008–1017, 2018.
- [9] Christian Daniel, Gerhard Neumann, Oliver Kroemer, and Jan Peters. Learning sequential motor tasks. In *IEEE International Conference on Robotics and Automation (ICRA)*, pages 2626–2632. IEEE, 2013.
- [10] Adrien Ecoffet, Joost Huizinga, Joel Lehman, Kenneth O Stanley, and Jeff Clune. Go-explore: a new approach for hard-exploration problems. *arXiv preprint arXiv:1901.10995*, 2019.
- [11] Georgios Gantamidis and Stavros Tripakis. Learning moore machines from input-output traces. In *21st Intl. Symposium on Formal Methods (FM)*, volume 9995 of *LNCS*, pages 291–309, 2016.
- [12] Robert Givan, Thomas L. Dean, and Matthew Greig. Equivalence notions and model minimization in Markov Decision Processes. *Artificial Intelligence*, 147(1-2):163–223, 2003.
- [13] Sergio Guadarrama, Anoop Korattikara, Oscar Ramirez, Pablo Castro, Ethan Holly, Sam Fishman, Ke Wang, Ekaterina Gonina, Neal Wu, Efi Kokiopoulou, Luciano Sbaiz, Jamie Smith, Gábor Bartók, Jesse Berent, Chris Harris, Vincent Vanhoucke, and Eugene Brevdo. TF-Agents: A library for reinforcement learning in tensorflow. 2018. [Online; accessed 25-June-2019].
- [14] Kaiming He, Xiangyu Zhang, Shaoqing Ren, and Jian Sun. Deep residual learning for image recognition. In *Proc. of the IEEE Conf. on Computer Vision and Pattern Recognition (CVPR)*, pages 770–778, 2016.
- [15] Andrew Hundt, Benjamin Killeen, Heeyeon Kwon, Chris Paxton, and Gregory D Hager. “Good robot!”: Efficient reinforcement learning for multi-step visual tasks via reward shaping. *arXiv preprint arXiv:1909.11730*, 2019.
- [16] Sergey Ioffe and Christian Szegedy. Batch normalization: Accelerating deep network training by reducing internal covariate shift. In *Intl. Conf. on Machine Learning (ICML)*, pages 448–456, 2015.

- [17] Dmitry Kalashnikov, Alex Irpan, Peter Pastor, Julian Ibarz, Alexander Herzog, Eric Jang, Deirdre Quillen, Ethan Holly, Mrinal Kalakrishnan, Vincent Vanhoucke, et al. Qt-opt: Scalable deep reinforcement learning for vision-based robotic manipulation. *arXiv preprint arXiv:1806.10293*, 2018.
- [18] Jonas Karlsson. Task decomposition in reinforcement learning. In *Proceedings of the AAAI Spring Symposium on Goal-Driven Learning*, 1994.
- [19] Ian Lenz, Honglak Lee, and Ashutosh Saxena. Deep learning for detecting robotic grasps. *The International Journal of Robotics Research*, 34(4-5):705–724, 2015.
- [20] Sergey Levine, Peter Pastor, Alex Krizhevsky, Julian Ibarz, and Deirdre Quillen. Learning hand-eye coordination for robotic grasping with deep learning and large-scale data collection. *The International Journal of Robotics Research*, 37(4-5):421–436, 2018.
- [21] Lihong Li, Thomas J. Walsh, and Michael L. Littman. Towards a unified theory of state abstraction for MDPs. In *International Symposium on Artificial Intelligence and Mathematics (ISAIM)*, 2006.
- [22] Josh Merel, Arun Ahuja, Vu Pham, Saran Tunyasuvunakool, Siqi Liu, Dhruva Tirumala, Nicolas Heess, and Greg Wayne. Hierarchical visuomotor control of humanoids. In *Proceedings of the 7th International Conference on Learning Representations, (ICLR)*, 2019.
- [23] Volodymyr Mnih, Koray Kavukcuoglu, David Silver, Andrei A. Rusu, Joel Veness, Marc G. Bellemare, Alex Graves, Martin A. Riedmiller, Andreas Fidjeland, Georg Ostrovski, Stig Petersen, Charles Beattie, Amir Sadik, Ioannis Antonoglou, Helen King, Dharshan Kumaran, Daan Wierstra, Shane Legg, and Demis Hassabis. Human-level control through deep reinforcement learning. *Nature*, 518(7540):529–533, 2015.
- [24] Andrew Y. Ng, Daishi Harada, and Stuart J. Russell. Policy invariance under reward transformations: Theory and application to reward shaping. In *Proceedings of the 16th International Conference on Machine Learning (ICML)*, pages 278–287, 1999.
- [25] Xue Bin Peng, Michael Chang, Grace Zhang, Pieter Abbeel, and Sergey Levine. MCP: Learning composable hierarchical control with multiplicative compositional policies. In *Advances in Neural Information Processing Systems (NeurIPS)*, pages 3686–3697, 2019.
- [26] Iyaylo Popov, Nicolas Heess, Timothy Lillicrap, Roland Hafner, Gabriel Barth-Maron, Matej Vecerik, Thomas Lampe, Yuval Tassa, Tom Erez, and Martin Riedmiller. Data-efficient deep reinforcement learning for dexterous manipulation. *arXiv preprint arXiv:1704.03073*, 2017.
- [27] Tim Salimans and Durk P Kingma. Weight normalization: A simple reparameterization to accelerate training of deep neural networks. In *Advances in Neural Information Processing Systems (NIPS)*, pages 901–909, 2016.
- [28] David Silver, Thomas Hubert, Julian Schrittwieser, Ioannis Antonoglou, Matthew Lai, Arthur Guez, Marc Lanctot, Laurent Sifre, Dharshan Kumaran, Thore Graepel, Timothy Lillicrap, Karen Simonyan, and Demis Hassabis. A general reinforcement learning algorithm that masters chess, shogi, and go through self-play. *Science*, 362(6419):1140–1144, 2018.
- [29] Richard S Sutton, Doina Precup, and Satinder Singh. Between MDPs and semi-MDPs: A framework for temporal abstraction in reinforcement learning. *Artificial Intelligence*, 112(1-2):181–211, 1999.
- [30] Rodrigo Toro Icarte, Torny Q. Klassen, Richard Valenzano, and Sheila A. McIlraith. Using reward machines for high-level task specification and decomposition in reinforcement learning. In *Proceedings of the 35th International Conference on Machine Learning (ICML)*, pages 2112–2121, 2018.
- [31] Rodrigo Toro Icarte, Ethan Waldie, Torny Klassen, Rick Valenzano, Margarita Castro, and Sheila McIlraith. Learning reward machines for partially observable reinforcement learning. In *Advances in Neural Information Processing Systems (NeurIPS)*, pages 15497–15508, 2019.

- [32] Ulrich Viereck, Andreas ten Pas andz Kate Saenko, and Robert Platt Jr. Learning a visuomotor controller for real world robotic grasping using simulated depth images. In *Proceedings of the 1st Annual Conference on Robot Learning (CoRL)*, pages 291–300, 2017.
- [33] Bohan Wu, Iretiayo Akinola, and Peter K. Allen. Pixel-attentive policy gradient for multi-fingered grasping in cluttered scenes. In *IEEE/RSJ IROS*, pages 1789–1796, 2019.
- [34] Jimmy Wu, Xingyuan Sun, Andy Zeng, Shuran Song, Johnny Lee, Szymon Rusinkiewicz, and Thomas Funkhouser. Spatial action maps for mobile manipulation. *arXiv preprint arXiv:2004.09141*, 2020.
- [35] Andy Zeng, Shuran Song, Johnny Lee, Alberto Rodriguez, and Thomas Funkhouser. Tossingbot: Learning to throw arbitrary objects with residual physics. *IEEE Transactions on Robotics*, 2020.
- [36] Andy Zeng, Shuran Song, Stefan Welker, Johnny Lee, Alberto Rodriguez, and Thomas Funkhouser. Learning synergies between pushing and grasping with self-supervised deep reinforcement learning. In *IEEE/RSJ Intl. Conference on Intelligent Robots and Systems (IROS)*, pages 4238–4245. IEEE, 2018.

Appendix

7.1 Detailed Experimental Setup

Environment implementation. We implemented the testing environments in OpenAI Gym, with the PyBullet physics engine. The environment consists of a *Universal Robot 5* (UR5) grasping arm, a plane, and several blocks of different colors that vary with the task. The robot is equipped with RGB and depth cameras with top-down views of the working area. Observations are RGB images with 320x160 pixels per channel. The robot can perform *pick* and *place* actions, parameterized with the pixel coordinates (x, y) of the target location of the end effector. The depth camera senses the depth of the objects in the scene, and is used to compute the height z of the target location.

Reward machine implementation. Reward machines are implemented as an OpenAI Gym class, and are used in conjunction with the environment to compute rewards. We implemented auxiliary functions to compute reward machines from a set of demonstrations, as explained in the paper.

DQN agents implementation. We implemented different versions of DQN in TF-agents [13]. In order to use TF-agents with OpenAI Gym environments and reward machines, we made use of wrappers.

Stacking blocks task. The stacking blocks task starts with two identical red blocks placed in random locations. The goal of the task is to stack one block on top of another.

Kitting task. The kitting task consists of three blocks of the same size but different colors—red, green, and blue—, and a container with three plates. One of the plates situated in one extreme of the container has a slightly different color. All objects are initially placed at a random location. The goal of the task is to place each block in their designated container: the red block should be placed inside of the distinct plate; the green block has to be placed in the middle plate; and the blue block has to be placed in the remaining plate.

Demonstrations. Demonstrations were handcrafted. They were generated with independent episodes, with objects initially placed in random locations. In the kitting task, we generated demonstrations that placed blocks in a fixed order: first the red block, then the green block, and finally the blue block. We found that this fixed order induced slightly better performance in DQRM, compared to using demonstrations that placed blocks in arbitrary order. We conjecture that this improved performance is due to the bias induced by demonstrations in the exploratory policy—which turns to be a good bias.

7.2 Detailed Model Architecture

ResNet network. In all cases, the DQN consists of two independent feed-forward 43-layer residual networks (ResNets) [14], each with a fully convolutional encoder-decoder architecture—one that outputs a dense pixel-wise prediction of Q values for picking, and the other for placing (see Figure 2 in the paper). Each pixel corresponds to an action (pick or place) executed at that respective location in the scene. Both ResNets jointly represent the Q function, to which the argmax of the predicted Q value maps returns a pick or place action from a greedy policy. This architecture has previously been shown to improve learning efficiency for vision-based DQNs [36, 15, 34], since Q value predictions are thereby spatially anchored on visual features—inducing translational equivariance (such that if an object to be picked in the scene is translated, then the picking action-values also translate).

Input observations. The four DQN agent configurations that we tested (namely, DQN, DQN(AS), DQN(RS), and DQRM) are fed with different input observations.

- In DQN, the input is a 3-channel RGB image with the top-down view of the scene. In the kitting task, the input to DQN has an additional 1-channel layer with a constant number tied with (but different from) the color of the block being held (or 255, if no block is held).
- In DQN(RS), the input is the same as in DQN.
- In DQN(AS), the input is the same as in DQN, plus N additional channels (as many as abstract states in the RM). The values of each channel are zero, except for the values of the channel tied with the current RM state, that are set to one—in other words, these N channels are one-hot channels that encode the current RM state.
- In DQRM, the input is the same as in DQN(AS).

Rewards. The reward given to each of the DQN configurations that we tested are different, depending on whether reward shaping is performed. In particular:

- In DQN, rewards are +0.5 if the MDP state transitions to a goal state, and zero otherwise. We set rewards to +0.5 and not to +1 because the range of the values that the ResNet can output is $[-0.5, +0.5]$.
- In DQN(RS), rewards are reshaped. Rewards to transitions (s, a, s') are the difference of potentials $\gamma Pot(s') - Pot(s)$. The potentials function $Pot(s) := \gamma^{dist(s)}$ is an exponential decay with the distance from s to the goal in the abstract planning graph. In practical terms, we set $Pot(s) = 1$ in goal states, as we suggested in the paper.
- In DQN(AS), rewards are the same as in DQN.
- In DQRM, rewards are the same as in DQN(RS).

Output actions. The agent outputs actions composed of the target (x, y, z) location of the gripper, together with a bit of information telling whether the action is *pick*, or *place*. Actions are computed from the Q value heatmaps of the ResNet networks. Each agent has two independent ResNet networks that output, respectively, heatmaps for the pick and place high-level planning actions. The planning action (pick or place) is selected from the heatmap that has the highest Q value. The control action—i.e., the low-level coordinates (x, y, z) with the target location of the gripper—are computed from the argmax of the heatmap $((x, y))$ and the z -coordinate of the object placed in the (x, y) location of the scene, obtained from the depth camera.

Training. Q predictions are optimized toward target Q values with Huber loss, trained with Adam and a learning rate of 10^{-5} , with a discount factor $\gamma = 0.7$. Training steps were performed each 8 exploration steps, with a batch size of 64. Unless otherwise noted, batch training was performed by sampling evenly from an experience replay buffer of size 1000, and a buffer of size 1000 fulfilled with demonstrations.

Data collection. We used an epsilon-greedy exploration policy, with $\epsilon = 0.3$. The exploration (and policy evaluation) horizon is 8 steps, after which the environment is reset.

Experience replay buffers. Each agent has two independent experience replay buffers. The first one is filled with demonstrations. The second one is filled with exploration data.